Classification of GLE and magnetospheric events through energy release of muons and neutrons: Observations by the SEVAN light detectors

A. Chilingarian, B.Sargsyan

Yerevan Physics Institute, Alikhanyan Brothers 2, Yerevan, Armenia 36

E mail chili987@gmail.com

Accepted: 08 May 2026

Abstract: The simultaneous detection of enhanced neutron and muon fluxes induced by solar energetic protons and by magnetospheric interactions marks a significant advance in our understanding and characterization of solar modulation effects. A new capability to record energy-release histograms represents an important improvement in instrumentation for monitoring cosmic-ray fluxes at the surface. Currently, the neutron monitor and SEVAN networks measure particle fluxes without directly assessing the incident particle energies. Energy-release histograms for neutrons and muons registered during Ground Level Enhancement (GLE) and Magnetospheric Enhancement (ME) events are markedly different. GLE releases extend well above 100 MeV, whereas ME events are limited to 10 MeV. New insights into the energy-release spectra of secondary particles enable us to characterize the types of solar events and provide constraints on the primary proton energies that initiate them, which is crucial for solar physics and space weather applications.

Key words:
Ground Level Enhancements, SEVAN light detector, neutron and muon spectroscopy, solar energetic particles

1. Introduction

The SEVAN light detector installed on the Aragats and Zugspitze mountains (Chilingarian et al., 2024a) has already demonstrated advantages in detecting solar events, including ground-level enhancements (GLEs, Poluianov et al., 2017), magnetospheric effects (MEs, Kudela et al., 2008), and Forbush decreases (FDs, Forbush, 1954).

The SEVAN light detector is a compact, cost-effective particle detector for space weather and atmospheric physics research (Chilingarian et al., 2022). It is the first detector capable of simultaneously measuring the count rates and energy deposits of both charged and neutral components of secondary cosmic rays. These measurements are crucial for studying:

- Thunderstorm Ground Enhancements (TGEs, Chilingarian et al., 2010; 2011), enabling energy spectrum reconstruction of electrons and gamma rays.
- Solar Energetic Particle (SEP) events and Ground Level Enhancements (GLEs), where muon and neutron enhancements carry information about primary proton energies.
- Forbush decreases (FDs), through the precise detection of cosmic ray flux suppression.
- Magnetospheric Effects (MEs) refer to the modulation of low-energy muons and neutrons by geomagnetic disturbances.

We compare the energy deposit histograms recorded by a 20 cm thick, 0.25 m² plastic scintillator at Aragats with a similar type that is 25 cm thick at Zugspitze. The comparison also considers a 1 m² veto scintillator above the spectrometric scintillator. At Aragats, the veto scintillator is 1 cm thick, while Zugspitze is 5 cm thick. The data acquisition electronics are identical at both locations. Logarithmic ADCs (LADC) enable measurements of energy releases over a wide range, reaching up to 300 MeV (Chilingarian et al., 2022).

The energy release histograms represent excess counts over background, distributed over 128 energy bins. The background counts were registered on fair weather before the solar events.

Table 1 summarizes the statistics of GLE and ME events and provides the hourly count rates at maximum intensity for events and locations. The maximum GLE flux occurred from 2:30 to 3:30 on May 11, 2024 (Chilingarian et al., 2024a), and ME from 11:00 to 12:00 on November 5, 2023 (Chilingarian et al., 2024b).

As shown in Table 1, the thousands of registered particles enable a reliable analysis and classification of solar events.

DOI: 10.31401/SunGeo.2026.01.01

Table 1. Summary table of muon and neutron energy release histograms observed during the GLE of May 11, 2024

Date	Location	Rc (GV)	Particle Type	Primary Type	Primary Energy (GeV)	Hourly Excess
11 May 2024	Zugspitze	3.7	Muons	SCR	8–10	10426
11 May 2024	Zugspitze	3.7	Neutrons	SCR	8–10	11232
5 November 2023	Zugspitze	3.7	All Particles	GCR	3.6	4658
11 May 2024	Aragats	7.1	Muons	SCR	8–10	7190
11 May 2024	Aragats	7.1	Neutrons	SCR	8–10	9631
5 November 2023	Aragats	7.1	All Particles	GCR	7.0	4102

At Zugspitze, the GLE total hourly excess for muons and neutrons exceeded 21,000 events, indicating a strong relativistic solar proton injection. Aragats, despite its higher geomagnetic rigidity (Rc = 7.1 GV), also recorded over 16,000 particles, demonstrating the penetration of high-energy solar cosmic rays. The neutron excess was slightly greater than muons at both sites, suggesting strong hadronic cascading. The hourly excesses of ME were notably lower, ranging from 4,100 to 4,600 particles, about four times less than in the GLE case. This reduced intensity corresponds with the low-energy nature of penetrating galactic cosmic rays with energies below Rc. The ME is driven by sub-cutoff GCRs transported into the middle atmosphere through magnetospheric processes. The form and scale of the histograms further confirm the absence of high-energy muon/neutron multiplicity during ME. This four-fold difference in the number of registered particles between GLE and ME events is not merely quantitative; it reflects a fundamental difference in physical origin, energy scale, and particle transport. SEVAN light's ability to resolve these differences across both muon and neutron channels serves as a strong diagnostic tool for:

- Discriminating between solar and magnetospheric events,
- Estimating primary energy and spectra of SEP events,
- Supporting atmospheric shower modeling with tools like CORSIKA to compare the observed energy-release histograms of atmospheric cascades with those initiated by monoenergetic primary protons.

This capability significantly advances solar event research and ground-based monitoring of space weather phenomena.

2. GLE 74 registered by the Mid-latitude NM and SEVAN networks

The geomagnetic storm (G5) of May 10-11, 2024, was among the most powerful in the past two decades (see Hayakawa et al., 2024). This event included a strong FD followed by GLE #74 during the recovery phase. Ground-based neutron monitors (Mavromichalaki et al., 2011) and the SEVAN network (Chilingarian et al., 2018) confirmed a GLE associated with 02:00 UTC on May 11, 2024, following an X5.8 flare that peaked at 01:23 UTC. However, Papaioannou et al. (2025) classify "all nonpolar stations as zero response" to the GLE event due to the simultaneous start of FD recovery and the magnetospheric effect. At both stations, Aragats and Lomnicky Stit, Neutron Monitors and the SEVAN detectors, GLE and FD were registered. Owing to this unique opportunity, in Figure 1, we demonstrate the FD recovery trend (dotted blue line) and the time series of Lomnicky Stit NM (blue) and SEVAN (green); the GLE enhancement is emphasized by a solid blue domain. Both time series from independent detectors explicitly show GLE against the background of the count-rate recovery after FD.

Around 15:00, we observe a peak in the SEVAN detector's count rate attributed to ground level enhancement (TGE, Chilingarian et al., 2010; 2011) – an abrupt burst of electrons and gamma rays from avalanches initiated by runaway electrons in a stormy atmosphere (Gurevich et al., 1992). This enhancement in count rate highlights the importance of monitoring atmospheric conditions to detect variations in count rate caused by external factors, including temperature, pressure, electric field, and FD recovery.

In Figure 2, we show the events registered by the Aragats Neutron Monitor (ArNM, red) and the SEVAN light detector (blue, neutrons, and green, muons; see details of detector operation in Chilingarian et al., 2024a). Again, we emphasize the FD recovery with a blue dotted line and the GLE with a solid blue domain. The neutron monitor and SEVAN detector register the GLE simultaneously and with a shape similar to that at Lomnicky Stit. Thus, at 2 stations with 2 different detectors, we obtain an analogous GLE enhancement and FD recovery trend.

The atmospheric conditions (outside temperature, red; atmospheric pressure, green), as illustrated in Fig. 3, remained relatively stable during FD and GLE. The time series of count rates from the largest Aragats Solar Neutron Spectrometer (ASNT; Chilingarian et al., 2022) is shown in blue. This instrument searches for direct neutrons emitted from solar flares. The second flux enhancement following the GLE is attributed to atmospheric pressure depletion.

Figures 1–3 demonstrate that GLE registration was genuine at middle latitudes and not an artifact of the rising FD phase. Multiple particle detectors at various sites indicate the GLE during FD recovery.

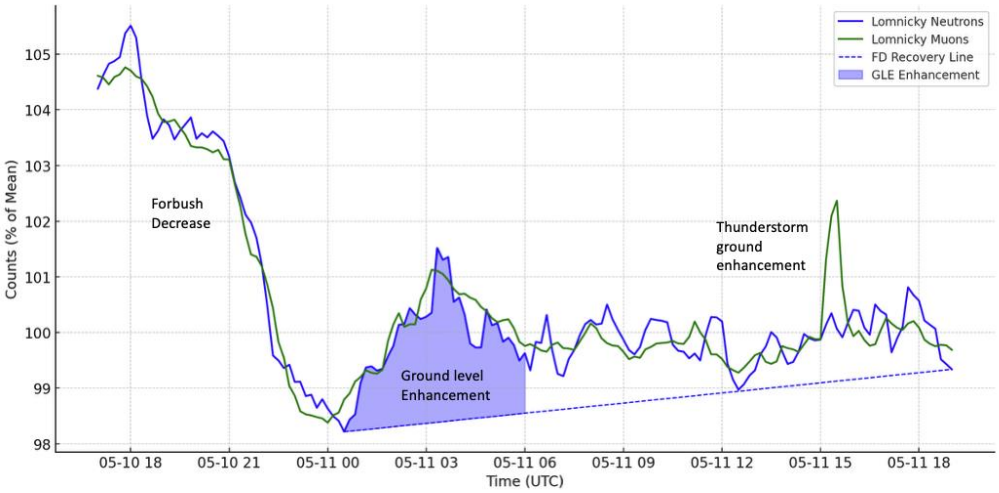

Figure 1. FD and GLE registered by Lomnicky Stit Neutron monitor (blue) and SEVAN detector's upper 5 cm thick scintillator (green). The dashed line indicates the recovery trend after FD; the shaded area is the GLE fluence.

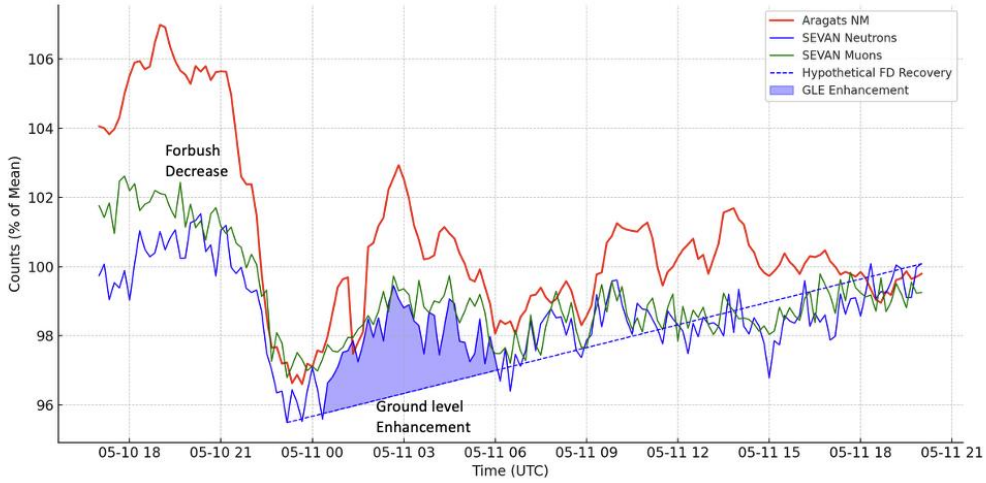

Figure 2. FD and GLE registered by the Aragats Neutron monitor (red) and SEVAN light detector: neutrons (blue) and muons (green). The dashed line indicates the recovery trend after FD; the shaded area is the GLE fluence.

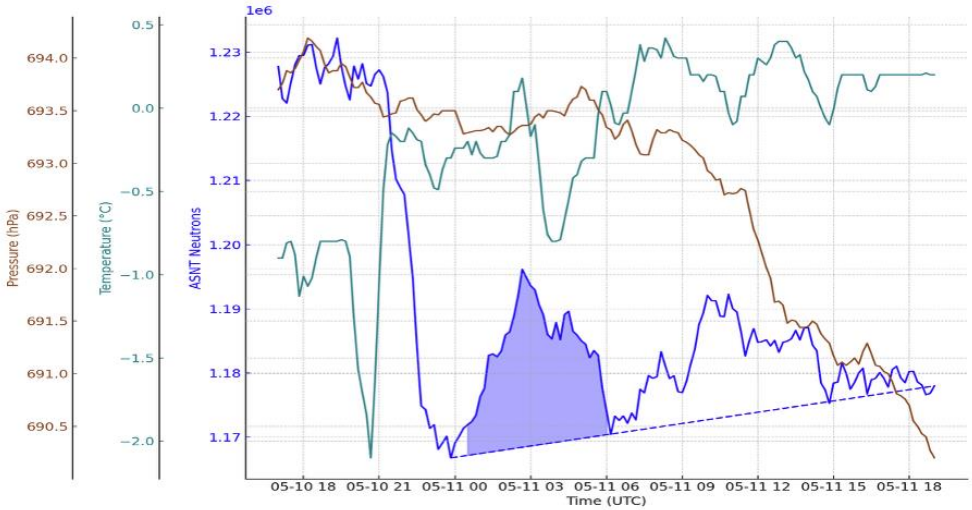

Figure 3. FD and GLE registered by Aragats Solar Neutron Telescope (ASNT, blue) and outside temperature (green), and atmospheric pressure (red). The dashed line indicates the recovery trend after FD; the shaded area is the GLE fluence.

3. Energy release histograms during GLE and ME events

Figure 4 presents energy release histograms for neutrons and muons simultaneously detected during the GLE at two observatories, Aragats (Rc = 7.1 GV) and Zugspitze (Rc = 3.7 GV), on May 11, 2024, from 2:30 to 3:30, capturing the maximum hourly flux of the GLE. Panel (a) shows muon energy releases recorded at Aragats during the May 11, 2024, event. The histogram distinguishes between electrons (0–25 MeV, black), single muons (25–60 MeV, blue), double muons (60–100 MeV, red), and multiple muons (>100 MeV, green). Panel (b) displays the corresponding neutron energy release spectrum from the same event, which is dominated by evaporation neutrons below 50 MeV. Panel (c) presents muon energy releases at Zugspitze for the same GLE. The spectrum here is shifted toward higher energies, with a dominant peak in the 100–250 MeV range, indicating a large number multiple muon events. Panel (d) shows the neutron spectrum from Zugspitze during the same event, again dominated by evaporation neutrons below 50 MeV.

The muon energy-release histograms provide a clearer distinction between single, double, and multiple coincidences than neutron spectra do. Simulations show that the contribution of low-energy muons is negligible. Thus, particles selected by the "11" coincidence and with energies below 25 MeV are dominated by electrons. The structured energy bands in the 25–60 MeV range can be attributed to electrons and single low-energy muons intersecting the detector at different angles (muon energy losses in 1 cm of scintillator are ≈ 2 MeV/cm). The 60–100 MeV interval can be attributed to double muons or more complicated interactions of high-energy muons in the spectrometer, and the >100 MeV domain – to muon bundles or again to interactions of high-energy muons. This capability is enabled by the well-defined energy deposition of minimum-ionizing muons, the spectrometer's extended energy range, and the 1 msec coincidence window, which effectively separates accidental coincidences or diffuse particle backgrounds. Multiple events recorded by the "01" neutral channel are subject to larger timing uncertainties, energy-dependent moderation effects, and overlapping thermal neutron captures, making it difficult to resolve distinct multiplicities of energy releases. Neutron spectra thus show a more continuous, smeared distribution, with limited ability to distinguish between single and multiple neutron events. This highlights the superior diagnostic power of muon spectrometry for characterizing the high-energy secondary particle structure during GLEs, particularly for correlating the energy-release pattern with primary energy.

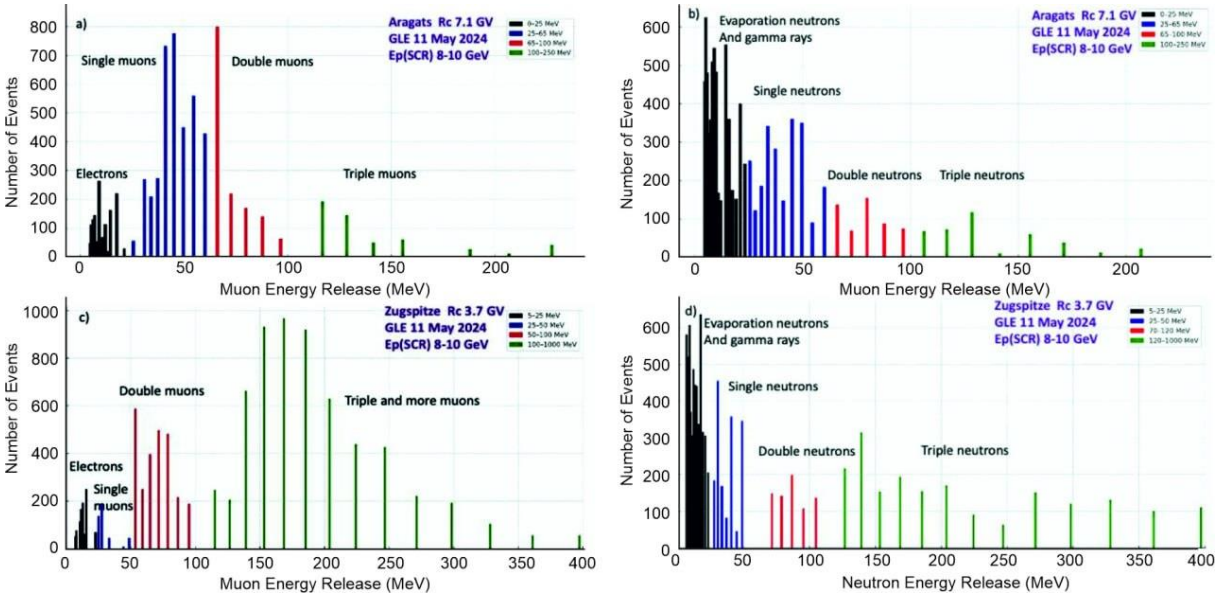

Figure 4. Energy release histograms of muons and neutrons recorded by the SEVAN light detector on Aragats (a and b) and Zugspitze (c and d)

These four panels highlight the contrast between muon and neutron energy-release signatures. Muon spectra (a, c) show broader distributions with significant high-energy components, especially at Zugspitze. Higher-multiplicity events demonstrate the cascading nature of cosmic-ray showers. In contrast, neutron spectra (b, d) are sharply peaked at low energies, consistent with production via nuclear evaporation and rapid thermalization. These differences underscore the diagnostic utility of particle-type-resolved measurements for distinguishing cosmic-ray primaries and assessing the energy content of GLEs. The observed differences in particle energy-release spectra between Aragats and Zugspitze reveal the effects of both geomagnetic cutoff rigidity and atmospheric depth on the development of secondary particles during GLEs. At Zugspitze (Rc = 3.7 GV, 2650 m altitude), a larger flux of GeV protons can access the atmosphere than at Aragats (Rc = 7.1 GV, 3200 m altitude). In particular, the muon spectrum at Zugspitze

(Fig. 4c) shows a strong excess in the 100–250 MeV range, dominated by higher-multiplicity muon events. This contrasts with Aragats (Fig. 4a), where the high-energy muon component is much weaker, and the spectrum is concentrated in 25–100 MeV. A similar trend is seen in the neutron spectra (Figs 4b and 4d), where Zugspitze exhibits a longer high-energy tail extending toward 200–300 MeV. In contrast, Aragats neutron releases fall off steeply beyond 100 MeV. These differences are primarily explained by geomagnetic filtering and shower development conditions. Once the primaries enter the atmosphere, the denser atmosphere above Zugspitze (~730 g/cm²) than at Aragats (~690 g/cm²) facilitates more extensive hadronic cascading and deeper shower development. This increases the probability that secondary muons and neutrons will reach the ground with higher energy releases. The third factor contributing to the observed differences is the scintillator thickness at the two sites. At Zugspitze, the detector is 25 cm thick, while at Aragats it is 20 cm. The thicker scintillator at Zugspitze increases the probability of full-energy deposition by traversing particles, especially for muons and neutrons with energies above several tens of MeV. As a result, due to the abundance of GeV protons, interactions in the thick atmosphere, and scintillator thickness, the measured energy-release spectrum at Zugspitze is extended to higher energies and shows many more multiple muon and neutron events.

Figure 5 presents energy release histograms for all detected particles (the separate energy release histograms in 2023 were not yet feasible) during the November 5, 2023, event at Aragats (a) and Zugspitze (b). In both cases, the energy distributions are narrowly confined between 5 and 11 MeV, symmetric, bell-shaped profiles centered around 8–9 MeV, and have no high-energy tails. Unlike the structured muon histograms from the May 11, 2024 GLEs, there is no separation into multiplicity groups, and no secondary particles exceed 20 MeV.

The expected proton energies for the magnetospheric events, i.e., galactic proton energies, fall slightly below the geomagnetic cutoffs at both sites, i.e., below 7.1 GeV at Aragats and 3.7 GeV at Zugspitze. Under normal magnetospheric conditions, such primary galactic protons would not reach the atmosphere. Observed histograms, which show much lower energies than in GLEs, confirm a magnetospheric effect caused by the interaction of approaching coronal mass ejections with the geomagnetic field, allowing sub-Rc protons to penetrate the middle atmosphere.

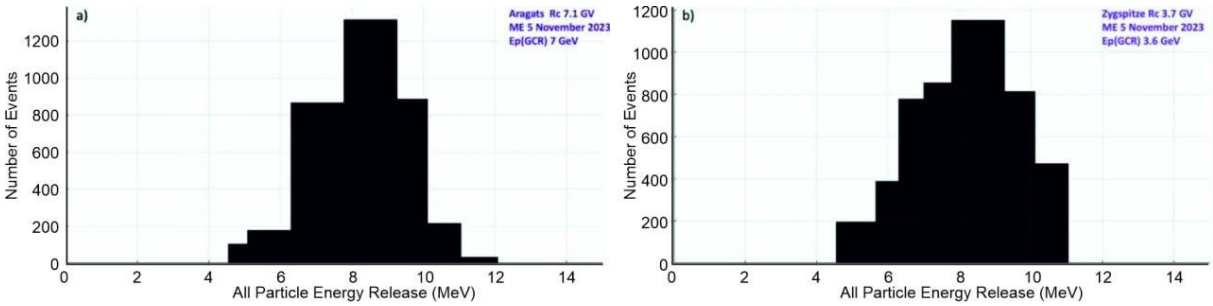

Figure 5. Energy release histograms of particles recorded by the SEVAN light detector on Aragats (a) and Zugspitze (b) on November 5, 2023

Compared to the May 2024 GLEs, which exhibited broad muon and neutron spectra extending well above 100 MeV and clear multiplicity structures, this event is much more limited and softer in spectral characteristics. The histogram shape suggests the presence of soft secondary particles, such as low-energy electrons, photons, and evaporation neutrons, likely generated by weak atmospheric cascades or sub-threshold interactions. This indicates that soft secondary populations dominate at both sites.

The similarity of the two spectra at Aragats and Zugspitze is compelling evidence of a large-scale magnetospheric phenomenon that:

- Partially suppressed geomagnetic rigidity filtering,
- Produces only soft, low-energy secondaries,
- Produces similar spectral shapes at both stations.

This reinforces the interpretation of the 5 November 2023 event as a magnetospheric disturbance, qualitatively distinct from traditional high-energy solar proton events.

4. Discussion and conclusions

The figure clearly demonstrates the presence of GLE at middle latitudes on May 11, 2024. FD's rising count rate did not dominate the count rate enhancement; it was rather weak, and the count rate recovered only two days after FD.

The absence of a high-energy tail clearly distinguishes this event from true solar GLEs, such as the one on 11 May 2024. Together, these cases demonstrate the power of energy-resolved neutron and muon spectroscopy to differentiate between solar and geomagnetic sources of secondary particle enhancements.

Our analysis of neutron monitors and SEVAN data from Lomnicky Stit and Aragats shows a similar pattern of deconvoluted GLE enhancement and FD recovery. Thus, the May 2024 GLE was reliably observed at mid-latitudes, as shown in Figures 1–2.

A comparison of the ME event of 5 November 2023 and the GLE event of 11 May 2024 reveals a striking divergence in the energy spectra of secondary particles reaching ground level. GLEs from solar relativistic protons (e.g., 11 May 2024) produce:

- Deep penetrating particle showers
- Distinct muon/neutron multiplicities
- Wide energy release spectra (0–300 MeV)

Magnetospheric enhancement events (e.g., 5 November 2023) produce:

- Low-energy soft secondaries
- No muon bundles or hard neutron components
- Spectrally narrow, symmetric histograms centered near 8–9 MeV

The ME event was caused by a decrease in the cutoff rigidity, allowing primary galactic protons with energies below the cutoff to penetrate the atmosphere and produce additional secondary particles, increasing the count rates of surface spectrometers. In contrast, the GLE event displays broad, structured energy spectra with distinct bands corresponding to multiple muon events and broadened neutron spectra that extend well above 100 MeV. These spectral shapes reflect relativistic secondary particles generated by solar energetic protons with primary energies exceeding the local geomagnetic cutoff, i.e., well above 7.1 GeV, probably 8-10 GeV. Thus, the absence of high-energy muons and structured multiplicity peaks distinguishes sub-threshold ME from super-threshold GLEs.

By comparing SEVAN light measurements with CORSIKA simulations of monoenergetic primary protons incident on Earth's atmosphere, the most probable SEP energies can be inferred. This reverse modeling approach links observed secondary energy spectra to the primary energy distribution, enabling a quantitative framework for assessing solar proton events in real time. In summary, the contrasting energy signatures of ME and GLE events, now clearly resolvable by SEVAN light, provide a new tool for solar and space weather physics. It connects ground-based observations with atmospheric cascade modeling, paving the way for a deeper understanding of the mechanisms and energies that drive particle enhancements in Earth's atmosphere.

References

Chilingarian A., Daryan A., Arakelyan K., Hovhannisyan A., Mailyan B., Melkumyan L., Hovsepyan G., and Vanyan L. 2010. Ground-based observations of thunderstorm-correlated fluxes of high-energy electrons, gamma rays, and neutrons, Phys Rev D. 82, 043009. doi.org/10.1103/PhysRevD.82.043009

Chilingarian A, Hovsepyan G., and Hovhannisyan A. 2011. Particle bursts from thunderclouds: Natural particle accelerators above our heads, Phys. Rev.. D 83, 062001. doi.org/10.1103/PhysRevD.83.062001

Chilingarian A., Babayan V., Karapetyan T., et al. (2018) The SEVAN Worldwide network of particle detectors: 10 years of operation, Advances in Space Research 61, 2680. https://doi.org/10.1016/j.asr.2018.02.030

Chilingarian A., Hovsepyan G., Karapetyan G., and Zazyan M. (2021) Stopping muon effect and estimating intracloud electric field, Astroparticle Physics 124 102505. https://doi.org/10.1016/j.astropartp

Chilingarian A., Hovsepyan G., Karapetyan T. et al. 2022. Measurements of energy spectra of relativistic electrons and gamma-ray avalanches developed in the thunderous atmosphere with Aragats Solar Neutron Telescope, Journal of Instrumentation, 17, P03002. doi 10.1088/1748-0221/17/03/P03002

Chilingarian A., Karapetyan T., Sargsyan B., Knapp J., Walter M., Rehm T. 2024a. Energy spectra of the first TGE observed on Zugspitze by the SEVAN light detector compared with the energetic TGE observed on Aragats, Astroparticle Physics 156, 02924. doi.org/10.1016/j.astropartphys.2024.102924

Chilingarian, A., Karapetyan, T., Sargsyan, B., Asatryan, K., Gabaryan, G. 2024b. Influence of magnetosphere disturbances on particle fluxes measured by ground-based detector, EPL, 148, 19001. doi:10.1209/0295-5075/ad7e4c

Chilingarian, A., Karapetyan, T., Sargsyan, B., Knapp, J., Walter, M., Rehm, T. (2024c). Increase in the count rates of ground-based cosmic-ray detectors caused by the heliomagnetic disturbance on 5 November 2023. EPL. doi: 10.1209/0295-5075/ad329c

Gurevich A. V., Milikh G. M., and Roussel-Dupre R. A. 1992. Runaway electron mechanism of air breakdown and preconditioning during a thunderstorm. Phys. Lett. 165A, 463. doi.org/10.1016/0375-9601(92)90348-P

Forbush S.E., World-Wide Cosmic-Ray Variations, 1937-1952, J. Geophys. Res., 59 (1954) 525. https://doi.org/10.1029/JZ059i004p00525

Hayakawa H., Ebihara Y., Mishev A., et al. 2025. The Solar and Geomagnetic Storms in 2024 May: A Flash Data Report. Astrophysical Journal 979, 49. https://doi.org/10.3847/1538-4357/ad95f4

Kudela K, Bučík R., and Bobík P.: 2008, On transmissivity of low energy cosmic rays in the disturbed magnetosphere, Advances in Space Research 42, 1300. https://doi.org/10.1016/j.asr.2007.02.00

Mavromichalaki H., Papaioannou A., Plainaki C., et al. 2011. Applications and usage of the real-time Neutron Monitor Database. Advances in Space Research 47, 2210–2222. https://doi.org/10.1016/j.asr.2010.02.019

Papaioannou, A., Mishev, A., Usoskin, I. et al. The High-Energy Protons of the Ground Level Enhancement (GLE74) Event on 11 May 2024. Sol Phys 300, 73 (2025). https://doi.org/10.1007/s11207-025-02486-0

Poluianov, S.V., Usoskin, I.G., Mishev, A.L., Shea, M.A., Smart, D.F. 2017, GLE and Sub-GLE Redefinition in the Light of High-Altitude Polar Neutron Monitors. Solar Phys. 292, 176.